

Design of polarization-insensitive multi-electrode GRIN lens with a blue-phase liquid crystal

Chao-Te Lee,^{1,2} Yan Li,¹ Hoang-Yan Lin,² and Shin-Tson Wu^{1,*}

¹College of Optics and Photonics, University of Central Florida, Orlando, Florida 32816, USA

²Institute of Photonics and Optoelectronics, National Taiwan University, Taipei 10617, Taiwan

*swu@mail.ucf.edu

Abstract: We report the design and simulation results of an adaptive GRIN lens based on multi-electrode addressed blue phase liquid crystal. A high dielectric constant layer helps to smoothen out the horizontal electric field and reduce the operating voltage. Such a GRIN lens is insensitive to polarization while keeping parabolic phase profile as the focal length changes.

©2011 Optical Society of America

OCIS codes: (230.3720) Liquid crystal devices; (110.1080) Active or adaptive optics.

References and links

1. S. Sato, "Liquid-crystal lens-cells with variable focal length," *Jpn. J. Appl. Phys.* **18**(9), 1679–1684 (1979).
2. T. Nose, S. Masuda, S. Sato, J. Li, L. C. Chien, and P. J. Bos, "Effects of low polymer content in a liquid-crystal microlens," *Opt. Lett.* **22**(6), 351–353 (1997).
3. M. G. H. Hiddink, S. T. de Zwart, O. H. Willemsen, and T. Dekker, "Locally switchable 3D displays," *Soc. Inf. Display Tech. Dig.* **37**(1), 1142–1145 (2006).
4. M. Ferstl and A. Frisch, "Static and dynamic Fresnel zone lenses for optical interconnections," *J. Mod. Opt.* **43**(7), 1451–1462 (1996).
5. P. F. McManamon, T. A. Dorschner, D. L. Corkum, L. J. Friedman, D. S. Hobbs, M. Holz, S. Liberman, H. Q. Nguyen, D. P. Resler, R. C. Sharp, and E. A. Watson, "Optical phased array technology," *Proc. IEEE* **84**(2), 268–298 (1996).
6. A. F. Naumov, M. Yu. Loktev, I. R. Guralnik, and G. Vdovin, "Liquid-crystal adaptive lenses with modal control," *Opt. Lett.* **23**(13), 992–994 (1998).
7. Y. Choi, J. H. Park, J. H. Kim, and S. D. Lee, "Fabrication of a focal length variable microlens array based on a nematic liquid crystal," *Opt. Mater.* **21**(1-3), 643–646 (2003).
8. H. Ren, Y. H. Fan, and S. T. Wu, "Tunable Fresnel lens using nanoscale polymer-dispersed liquid crystals," *Appl. Phys. Lett.* **83**(8), 1515–1517 (2003).
9. H. Ren, Y. H. Fan, and S. T. Wu, "Liquid-crystal microlens arrays using patterned polymer networks," *Opt. Lett.* **29**(14), 1608–1610 (2004).
10. Y. H. Fan, H. Ren, X. Liang, H. Wang, and S. T. Wu, "Liquid crystal microlens arrays with switchable positive and negative focal lengths," *J. Display Technol.* **1**(1), 151–156 (2005).
11. H. Ren, D. W. Fox, B. Wu, and S. T. Wu, "Liquid crystal lens with large focal length tunability and low operating voltage," *Opt. Express* **15**(18), 11328–11335 (2007).
12. Y. P. Huang, C. W. Chen, and T. C. Shen, "High resolution autostereoscopic 3D display with scanning multi-electrode driving liquid crystal (MeD-LC) Lens," *Soc. Inf. Display Tech. Digest* **40**(1), 336–339 (2009).
13. Y. Y. Kao, P. C. P. Chao, and C. W. Hsueh, "A new low-voltage-driven GRIN liquid crystal lens with multiple ring electrodes in unequal widths," *Opt. Express* **18**(18), 18506–18518 (2010).
14. H. Kikuchi, M. Yokota, Y. Hisakado, H. Yang, and T. Kajiyama, "Polymer-stabilized liquid crystal blue phases," *Nat. Mater.* **1**(1), 64–68 (2002).
15. Y. Haseba, H. Kikuchi, T. Nagamura, and T. Kajiyama, "Large electro-optic Kerr effect in nanostructured chiral liquid-crystal composites over a wide temperature range," *Adv. Mater. (Deerfield Beach Fla.)* **17**(19), 2311–2315 (2005).
16. Z. Ge, S. Gauza, M. Jiao, H. Xianyu, and S. T. Wu, "Electro-optics of polymer-stabilized blue phase liquid crystal displays," *Appl. Phys. Lett.* **94**(10), 101104 (2009).
17. L. Rao, Z. Ge, S. T. Wu, and S. H. Lee, "Low voltage blue-phase liquid crystal displays," *Appl. Phys. Lett.* **95**(23), 231101 (2009).
18. K. M. Chen, S. Gauza, H. Xianyu, and S. T. Wu, "Submillisecond gray-level response time of a polymer-stabilized blue-phase liquid crystal," *J. Display Technol.* **6**(2), 49–51 (2010).
19. Y. H. Lin, H. S. Chen, H. C. Lin, Y. S. Tsou, H. K. Hsu, and W. Y. Li, "Polarizer-free and fast response microlens arrays using polymer-stabilized blue phase liquid crystals," *Appl. Phys. Lett.* **96**(11), 113505 (2010).
20. Y. Li and S. T. Wu, "Polarization independent adaptive microlens with a blue-phase liquid crystal," *Opt. Express* **19**(9), 8045–8050 (2011).

21. D. Mardare and G. Rusu, "Comparison of the dielectric properties for doped and undoped TiO₂ thin films," *J. Optoelectron. Adv. Mater.* **6**, 333–336 (2004).
22. J. Yan, H. C. Cheng, S. Gauza, Y. Li, M. Jiao, L. Rao, and S. T. Wu, "Extended Kerr effect of polymer-stabilized blue-phase liquid crystals," *Appl. Phys. Lett.* **96**(7), 071105 (2010).
23. L. Rao, J. Yan, S. T. Wu, S. Yamamoto, and Y. Haseba, "A large Kerr constant polymer-stabilized blue phase liquid crystal," *Appl. Phys. Lett.* **98**(8), 081109 (2011).
24. A. Lien, "Extended Jones matrix representation for the twisted nematic liquid-crystal display at oblique incidence," *Appl. Phys. Lett.* **57**(26), 2767–2769 (1990).
25. Z. Ge, T. X. Wu, X. Zhu, and S. T. Wu, "Reflective liquid-crystal displays with asymmetric incident and exit angles," *J. Opt. Soc. Am. A* **22**(5), 966–977 (2005).

1. Introduction

Adaptive liquid crystal (LC) lens offers a tunable focal length and is useful for auto-focusing [1, 2], 2D/3D switchable displays [3], and tunable photonic devices [4, 5]. Two types of adaptive LC lenses have been developed: lenticular lens and gradient-index (GRIN) lens. The latter is more attractive because it uses planar surface structure and has less LC alignment issues [6]. Several approaches for generating gradient refractive index in a nematic LC have been demonstrated [6–13]. Among them, multi-electrode structure [12, 13] enables finer phase control for producing nearly ideal parabolic phase profile. However, conventional nematic LC lens requires two orthogonally oriented cells to overcome the polarization dependency. Moreover, the response time is relatively slow, especially when a thick LC layer is used for obtaining a short focal length.

To overcome the abovementioned problems in nematic LC devices, polymer-stabilized blue-phase liquid crystal (BPLC) based on Kerr effect has been proposed [14–17]. BPLC exhibits submillisecond gray-to-gray response time [18] and it does not require LC alignment layer. A hole-patterned microlens using polymer-stabilized BPLC has been recently demonstrated experimentally [19]. However, this lens has a compromised image quality due to non-ideal phase shape, and the two orthogonal polarizations possess a slightly different focal length because of the strong horizontal electric fields near the edge of the hole. A polarization independent BPLC lens based on concave (or convex) electrodes has also been proposed [20], but it requires sophisticated fabrication process and precise control of the electrode shape.

In this paper, we utilize a multi-electrode structure to control the lens phase profile and a high dielectric constant (ϵ) layer to achieve low voltage operation. A conventional transparent dielectric material TiO₂ has $\epsilon = 80$, whereas the TiO₂ film doped with 0.35 at. % Nb can reach $\epsilon = 311$, or doped with 0.4 at. % Ce can reach $\epsilon = 120$ [21]. Our simulation results show that the proposed BPLC lens is polarization insensitive while keeping parabolic-like phase profile during focus switching.

2. Design and device configuration

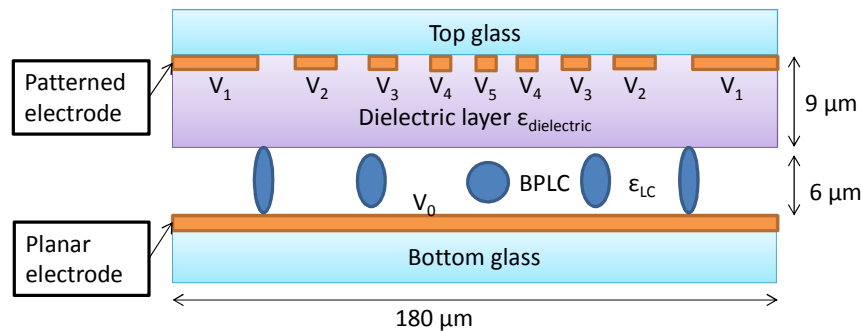


Fig. 1. Cross section of the proposed multi-electrode BPLC lens.

Figure 1 shows the side-view of our proposed BPLC lens. It consists of a multi-electrode structure over-coated with a 9-μm-thick high dielectric constant material. The bottom

substrate has a planar ITO (indium tin oxide) electrode on the inner side. The cell gap and diameter of the BPLC lens is 6 μm and 180 μm , respectively. In Fig. 1, the electrode width from the edge to the center (i.e., with the voltages from V_1 to V_5) is 25, 7, 5, 3 and 2 μm , and the distance between each electrode is about 12 μm on the top substrate. All the electrodes are assumed to have 0.04 μm in height.

In the proposed structure, when $V_0 = V_1 = V_2 = V_3 = V_4 = 0$, the BPLC is optically isotropic and does not contribute to any phase change. As the applied voltage increases, vertical electric fields are generated in the BPLC layer. Based on the Extended Kerr model [22], the induced birefringence is proportional to electric field (E) as shown in Eq. (1):

$$\Delta n_{\text{induced}}(E) = \Delta n_s [1 - \exp(-(E/E_s)^2)], \quad (1)$$

where Δn_s is the saturation induced birefringence and E_s is the saturation electric field of the BPLC composite. For a normally incident light, it experiences an ordinary refractive index which depends on E as

$$n_o(E) \approx n_{\text{iso}} - \Delta n_{\text{induced}}(E)/3, \quad (2)$$

regardless of polarization, provided that horizontal field does not exist. In Eq. (2), n_{iso} is the refractive index in the isotropic state, i.e., $E = 0$. In our device, the bottom planar electrode is always grounded ($V_0 = 0$). In order to obtain a positive lens and high efficiency, the electric field should be kept at zero at the lens center. Thus, we set $V_5 = 0$. Meanwhile, to obtain the desired parabolic phase profile the voltage from the center to the edge electrodes should increase gradually.

The importance of the dielectric layer is twofold: 1. On the top substrate, each electrode will cause a drastic voltage change near the electrode, so it needs a dielectric layer to smoothen out the phase profile. 2. The horizontal electric field produced between two top electrodes is very strong near the electrodes, thus, it will cause polarization dependence for the lens. On the other hand, higher dielectric constant of the dielectric layer is preferred. For a large Kerr constant BPLC (Kerr constant $K \approx \Delta n_s / \lambda E_s^2 = 10 \text{ nm/V}^2$), its dielectric constant is often large. For example, Chisso JC-BP01M has a dielectric constant $\epsilon_{LC} \sim 45$ in the voltage-off state [23]. The employed dielectric layer and BPLC layer can be treated as serial capacitors, and the applied voltage is divided into two terms:

$$V_{\text{total}} = V_{\text{BPLC}} + V_{\text{dielectric}} = \frac{Q}{C_{\text{BPLC}}} + \frac{Q}{C_{\text{dielectric}}}. \quad (3)$$

In Eq. (3), V_{total} is the voltage between two electrodes on the top and bottom substrate, V_{BPLC} and $V_{\text{dielectric}}$ stand for the voltage on the BPLC and dielectric layer, respectively; Q is the accumulated electric charge, and C_{BPLC} and $C_{\text{dielectric}}$ are the capacitances of BPLC and dielectric layer, which are proportional to the dielectric constant ϵ_{LC} and $\epsilon_{\text{dielectric}}$. For a given V_{total} and ϵ_{LC} , a high $\epsilon_{\text{dielectric}}$ in Fig. 1 helps to obtain a high V_{BPLC} . Undoped TiO_2 is an attractive candidate because of its high transparency and large dielectric constant (~ 80). It can also be prepared by sol-gel process to obtain a thicker film. With a proper doping, the dielectric constant of TiO_2 can be enhanced to be over 120 [21]. Thus, in next section we use $\epsilon_{\text{dielectric}} = 80$ and 120 in our simulations and compare their performances.

3. Simulation results

We use a commercial software Techwiz (Sanayi, Korea) to compute the electric potential distribution and then calculate the optical properties based on extended 2x2 Jones Matrix [24,25]. Let us assume the BPLC has $\Delta n_s \sim 0.2$ (at $\lambda = 550 \text{ nm}$), $E_s \sim 5.6 \text{ V}/\mu\text{m}$, and Kerr constant $K \approx \Delta n_s / \lambda E_s^2 = 11.5 \text{ nm/V}^2$, which is similar to the data reported in [22].

Figure 2 shows the simulated relative phase profiles of the proposed GRIN lens with $\epsilon_{LC} = 45$ and $\epsilon_{\text{dielectric}} = 80$. The electrode voltages V_1, V_2, V_3, V_4 and V_5 are 75V, 44V, 26V, 13V and 0V, respectively. We only examine the central 150 μm (from $-75 \mu\text{m}$ to $+75 \mu\text{m}$) of the lens.

Beyond this region, the lens fringe is not parabolic anymore. For convenience, we set the phase at center of lens to be zero. To investigate the polarization effect, we plot the relative phase profiles for e-wave (red line) and o-wave (blue line), as compared to the ideal parabolic shape (black line). For the lens locations at around $\pm 60\mu\text{m}$, the maximum phase difference between e-wave and o-wave is less than 0.036π . The phase difference of the center and the edge for proposed structure is 1.1π . For the structure without dielectric layer in Fig. 1, the total phase difference will be 1.4π between the center and the edge. This is because the dielectric layer shields part of the voltage according to Eq. (3). Moreover, the proposed structure also creates good parabolic phase shapes for both e-wave and o-wave within $\pm 10\%$ tolerance of the parabolic line. This implies that such a BPLC lens is polarization insensitive.

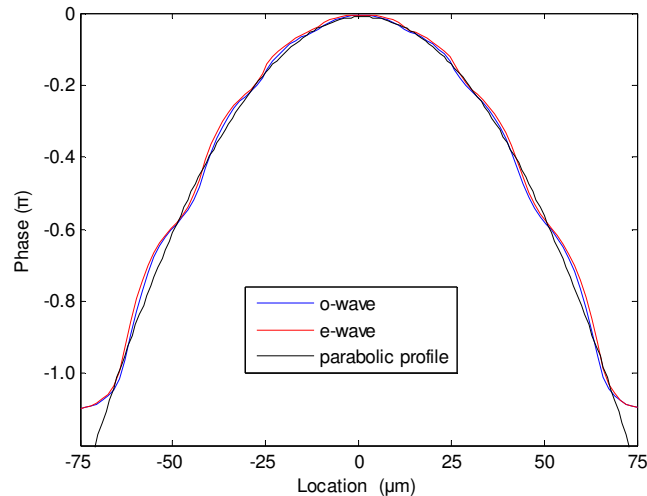


Fig. 2. Simulated phase profiles across the central $150\mu\text{m}$ of the lens for e-wave, o-wave, and ideal parabolic shape.

Next, we change the dielectric constant $\epsilon_{dielectric}$ from 80 to 120. To obtain the same phase change and profile, we adjust the voltages from V_1 to V_5 to be 65V, 38V, 22V, 11V and 0V; other parameters stay unchanged. Results are shown in Fig. 3(a). The maximum phase difference is still 1.1π which is almost the same as that in Fig. 2. However, the required maximum voltage is reduced from 75V to 65V because of the reduced voltage shielding effect. Also, the phase profile matches well (within $\pm 9\%$) with the parabolic profile (black line) in Fig. 3(a). For the lens locations at around $\pm 60\mu\text{m}$, the maximum phase difference between e-wave and o-wave is less than 0.032π . Moreover, we decrease the maximum voltage from 65V to 25V to alter the phase difference and focal length. To fit the parabolic phase profile, the voltages from V_1 to V_5 subsequently become 25V, 18V, 10.8V, 5.5V and 0V. From Fig. 3(b), the maximum phase difference is 0.28π . Although the e-wave (red line) and o-wave (blue line) phase profile in Fig. 3(b) is not as good as 3(a), it still remains within $\pm 11\%$ tolerance as compared to the parabolic line (black line). Figure 3(b) also shows a good consistency between e-wave and o-wave. For the lens locations at around $\pm 60\mu\text{m}$, the maximum phase difference between e-wave and o-wave is less than 0.004π . In our design, higher operating voltage tends to have better phase profile. Table 1 summarizes the voltage dependence of phase and focal length. The voltages from V_1 to V_4 are chosen to fit the parabolic phase profile. They can be digitally controlled to minimize the aberrations. In Table 1, the radii and phases are indicated to fit the parabolic phase profiles, note that it is not the same as the diameter described in Fig. 1. And the focal length can be calculated from following equation:

$$f = \frac{R^2}{2\delta n(E)d_{LC}}, \quad (4)$$

where $\delta n(E)$ is the index difference between the lens center and edge, R is the radius of the lens, and d_{LC} is the BPLC layer thickness.

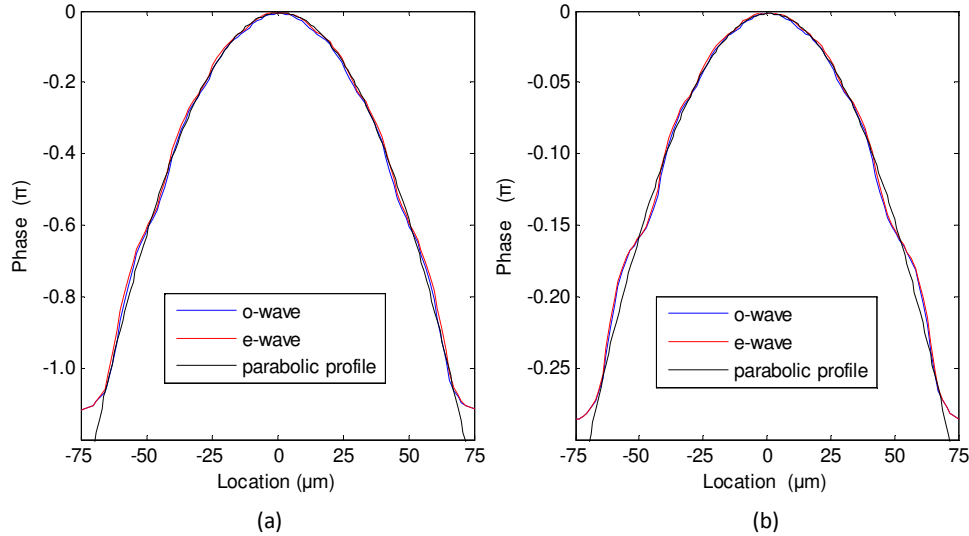


Fig. 3. Simulated phase profile of the BPLC lens with $\epsilon_{dielectric} = 120$. (a) The maximum voltage is 65V, resulting in 1.1π phase difference. (b) The maximum voltage is 25V, resulting in 0.28π phase difference.

Table 1. Simulated Phase and Focal Length at Different Operating Voltages.

Radius (μm)	V_1 (Volt)	V_2 (Volt)	V_3 (Volt)	V_4 (Volt)	Phase (π)	Effective Focal length (mm)
65	65.0	38.2	22.3	11.0	1.05	7.32
65	55.0	33.0	19.8	9.9	0.90	8.77
65	45.0	29.7	17.6	8.6	0.70	11.31
65	35.0	24.5	14.4	7.0	0.49	16.66
65	25.0	18.0	10.8	5.5	0.26	29.21
65	21.0	15.5	9.2	4.8	0.20	38.41
65	15.0	11.3	6.8	3.6	0.11	72.00

Briefly, we summarize the important points for optimizing the proposed structure: For a GRIN BPLC lens, a dielectric layer is inevitable to shield the horizontal electric field. A thicker dielectric layer will lead to a better consistence for e-wave and o-wave. In addition, the proposed multi-electrode structure needs a dielectric layer to smoothen the voltage around each electrode on the top substrate. However, this dielectric layer will also shield the voltage applied to the BPLC layer according to Eq. (3). Therefore, a high- ϵ dielectric layer is preferred. On the other hand, if the operating voltages, the dielectric layer thickness, and the BPLC thickness are all fixed, and the multi-electrode pattern remains the same line/space ratios, then the larger the lens diameter is, the more consistent the e-wave and o-wave are. This is because the vertical field has stronger effect than horizontal one in this case. However, it is hard to maintain parabolic phase profile if the gaps between electrodes on the top substrate keep on increasing. Otherwise the number of electrodes has to be increased. Also the phase profile can be optimized further by increasing the number of electrodes. But it requires more addressing voltages.

Figure 4 shows the voltage-dependent focal length for the lens structure in Fig. 1. The “voltage” in Fig. 4 means the maximum voltage among electrodes. The black curve (squares) is for dielectric layer with $\epsilon_{dielectric} = 80$, whereas the red one (circles) is for $\epsilon_{dielectric} = 120$. At a given voltage, the multi-electrode structure with $\epsilon_{dielectric} = 120$ keeps a somewhat shorter focal length. As expected from Eq. (4), the focal length gets shorter as the voltage increases. For each data point in Fig. 4, since the e-wave and o-wave are consistent and have the same phases at the center and the edge, their focal length would be the same. In the low voltage region, the change of focal length is more dramatic, while in the high voltage region the slope becomes flatter. Similar results and explanation can be found in [20].

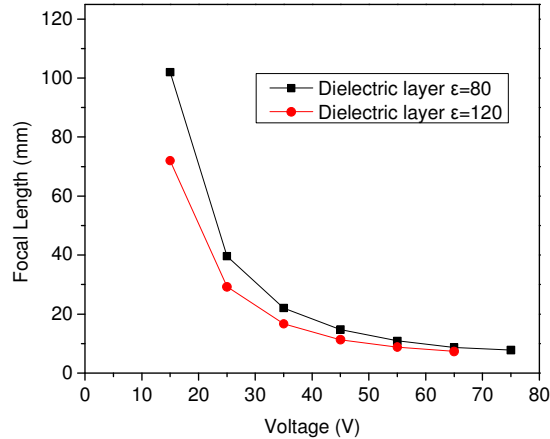


Fig. 4. Simulated voltage-dependent focal length of the multi-electrode BPLC lens with $\epsilon_{dielectric} = 80$ and 120.

3. Conclusion

We present a new design of multi-electrode BPLC lens to achieve polarization insensitivity and parabolic phase profile. The operating voltages can be digitally controlled to varying the focal length from 7.32mm to infinity. Even though at low operating voltages, the proposed structure can still maintain good consistence between e-wave and o-wave, and parabolic phase shape. By placing higher dielectric constant material for dielectric layer, the operating voltages can be further reduced. Since it is a layer-by-layer structure, the fabrication method can be easily carried out by the existing lithography process for LCDs. Simulation results show that this device is insensitive to the polarization throughout the whole focal lengths. Such a device has potential applications for polarization insensitive photonics and displays.

Acknowledgements

The authors are indebted to Jin Yan, Su Xu and Yifan Liu for useful discussion.